Journal for ImmunoTherapy of Cancer

WWOX tuning of oleic acid signaling orchestrates immunosuppressive macrophage polarization and sensitizes hepatocellular carcinoma to immunotherapy

Shaoqing Liu,[1] Shiguang Yang,[2] Min Xu,[1] Qiang Zhou,[1] Jialei Weng,[1] Zhiqiu Hu,[2] Minghao Xu,[1] Wenxin Xu,[1] Yong Yi,[1] Yi Shi,[3] Qiongzhu Dong,[2] Mien-Chie Hung ,[4] Ning Ren ,[1] Chenhao Zhou[1]

To cite: Liu S, Yang S, Xu M, *et al*. WWOX tuning of oleic acid signaling orchestrates immunosuppressive macrophage polarization and sensitizes hepatocellular carcinoma to immunotherapy. *Journal for ImmunoTherapy of Cancer* 2024;**12**:e010422. doi:10.1136/jitc-2024-010422

► Additional supplemental material is published online only. To view, please visit the journal online (https://doi.org/10.1136/jitc-2024-010422).

SL, SY and MX contributed equally.

Accepted 13 October 2024

Check for updates

© Author(s) (or their employer(s)) 2024. Re-use permitted under CC BY-NC. No commercial re-use. See rights and permissions. Published by BMJ.

For numbered affiliations see end of article.

Correspondence to
Dr Chenhao Zhou;
zhouchenhao@fudan.edu.cn

Dr Mien-Chie Hung;
mhung@cmu.edu.tw

Dr Ning Ren;
ren.ning@zs-hospital.sh.cn

ABSTRACT

Background Immune checkpoint inhibitors (ICIs) are therapeutically effective for hepatocellular carcinoma (HCC) but are individually selective. This study examined the role of specific common fragile sites (CFSs) related gene in HCC immunotherapy.

Methods We analyzed HCC tissues using next-generation sequencing and flow cytometry via time-of-flight technology. A humanized orthotopic HCC mouse model, an in vitro co-culture system, untargeted metabolomics and a DNA pulldown assay were used to examine the function and mechanism of WWOX in the tumor immune response.

Results WWOX was the most upregulated CFS-related gene in HCC patients responsive to ICIs. WWOX deficiency renders HCC resistant to PD-1 treatment in humanized orthotopic HCC mouse model. Macrophage infiltration is increased and CD8 T-cell subset infiltration is decreased in WWOX-deficient HCC patients. HCC-derived oleic acid (OA) promotes macrophage conversion to an immunosuppressive phenotype. Mechanistically, WWOX deficiency promoted OA synthesis primarily via competitive binding of NME2 with KAT1, which promoted acetylation of NME2 at site 31 and inhibited NME2 binding to the SCD5 promoter region. Pharmacological blockade of SCD5 enhanced the antitumor effects of anti-PD-1 therapy.

Conclusions WWOX is a key factor for immune escape in HCC patients, which suggests its use as a biomarker for stratified treatment with ICIs in clinical HCC patients.

WHAT IS ALREADY KNOWN ON THIS TOPIC

⇒ Hepatocellular carcinoma (HCC) is one of the most malignant tumors with a high recurrence rate and poor prognosis. Immunotherapy has emerged as an alternative therapy for HCC. Targeting the immune microenvironment significantly improves therapeutic efficacy in immune checkpoint inhibitors. WWOX was a tumor suppressor, and it was involved in a variety of biological processes. However, its effects on tumor immune microenvironment and immunotherapy efficacy are unknown.

WHAT THIS STUDY ADDS

⇒ WWOX expression is elevated in HCC tumors and serum from patients who respond to anti-PD-1 therapy. WWOX deficiency increases the infiltration of immunosuppressive macrophages in vivo. HCC cell-intrinsic WWOX suppresses macrophage migration and immunosuppressive polarization by inhibiting tumor cell-derived oleic acid signaling. WWOX/NME2/SCD5 axis can promote the secretion of oleic acid by tumor cells. Blockade of SCD5 signaling enhanced the therapeutic effect of anti-PD-1 therapy.

HOW THIS STUDY MIGHT AFFECT RESEARCH, PRACTICE OR POLICY

⇒ These insights highlight the promising application of WWOX as a predictive biomarker for immunotherapy response and the importance of SCD5 blockade as a promising therapeutic target for enhancing immunotherapy efficacy in HCC patients.

BACKGROUND

Primary liver cancer is the sixth most commonly diagnosed cancer and the third-leading cause of cancer death, with the highest incidence in Asia.[1] Hepatocellular carcinoma (HCC) is the most common type of primary liver cancer and accounts for approximately 75% of all cases.[2] There are various treatments for HCC, including surgical resection, liver transplantation and local ablation, which are primarily used in the early stage, and systemic treatment is mostly used in advanced-stage patients.[3 4] However, approximately 80% of patients have advanced HCC at the time of initial diagnosis, and the 5-year survival rate is less than 18% due to numerous factors, such as poor response to medication and susceptibility to recurrence.[4–6] Immunotherapy, represented by immune checkpoint inhibitors (ICIs), such as nivolumab and pembrolizumab, has emerged

as an alternative therapy for HCC, and these agents exert antitumor effects primarily by promoting T-cell initiation and activation.[7] Clinical studies have shown that ICIs, such as nivolumab, significantly improve the overall survival (OS) of drug-resistant patients and have gradually become the preferred drug treatment option.[8 9] However, the overall uneven therapeutic efficacy of ICIs and the obvious phenomenon of drug resistance have made the development of effective efficacy-predicting biomarkers a clinical problem that must be solved.

The immune system plays an important biological role in tumor progression.[10] Impairment of the tumor immune system promotes tumor progression by generating a tumor-immunosuppressive microenvironment, which leads to immune escape.[11] The tumor immune microenvironment (TIME) in HCC is primarily composed of tumor cells, immune cells and other components, and tumor-associated macrophages (TAMs) play important roles in the metastasis and drug resistance of HCC.[12] TAMs primarily consist of M1 (induced by IFNγ alone or with Lipopolysaccharide) and M2 (induced by IL-4 and IL-13) macrophages, and M2 macrophages mediate the Th2 response and promote tumor progression in a direct and indirect manner, respectively.[13–15] Therefore, targeting M2 macrophage recruitment and clearance may be a new tumor therapeutic strategy. Complex factors affect the polarization fate of TAMs, and further elucidation of the mechanism of TAM polarization has important clinical significance for HCC treatment.

Common fragile sites (CFSs) are normal chromosomal regions prone to forming gaps or breakages on partial inhibition of DNA synthesis, which correlate with chromosomal rearrangement and copy number variation.[16] FRA3B and FRA16D are the two most classical fragile sites, most frequently expressed and best characterized in tumor cells, and both are located within fragile histidine triad and WW domain-containing oxidoreductase (WWOX) genes, respectively.[17] Our previous study revealed that the WWOX rs9926344 polymorphism was associated with the recurrence of HCC.[18] Previous studies showed that WWOX was a tumor suppressor that may be involved in a variety of biological processes, including cell proliferation, metastasis and metabolism.[19 20] However, few studies focused on the biological role of CFS-related genes, especially classical genes, in HCC tumor immunity. By analyzing the transcriptome profiles of HCC patients with or without response to ICIs, we identified WWOX as an effective predictor of ICI response. Furthermore, we used in vitro experiments and a humanized mouse model of HCC and determined that the molecular mechanism of WWOX-mediated immunosensitization may originate from significant inhibition of the NME2/SCD5/oleic acid (OA) axis.

METHODS

Patients and specimens

We retrospectively collected pretreatment serum from 57 HCC patients who underwent PD-1 antibody therapy from September 2019 to March 2022 at Zhongshan Hospital of Fudan University. According to the Solid Tumor Response Evaluation Criteria,[21] PD-1 antibody-responsive patients (n=28) were defined as having a complete remission on imaging assessment or a partial remission of >6 months, whereas PD-1 antibody-resistant patients (n=29) were defined as having stable disease or disease progression. Among them, tumor tissues from 4 PD-1 responder and 4 PD-1 non-responder were used for RNA sequencing. The clinicopathological characteristics of these patients are shown in online supplemental table 1.

Meanwhile, we continued to retrospectively collect 176 tumor tissues from HCC patients who visited Zhongshan Hospital of Fudan University from January 2009 to January 2010 for immunohistochemical (IHC) staining. Patient inclusion criteria and follow-up were as previously described.[22] The clinicopathological characteristics and follow-up of these patients are shown in online supplemental tables 3 and 4.

More materials and methods details are available in online supplemental file 1.

RESULTS

WWOX mediates the resistance of HCC to anti-PD-1 treatment

We first performed next-generation sequencing (NGS) on eight HCC biopsy samples from patients with different ICI responses (online supplemental table 1). Single-sample genomic enrichment analysis (ssGSEA) revealed differences in tumor immunoreactivity between the two groups (online supplemental figure 1A). Differential analysis revealed WWOX was the most upregulated CFS related gene in ICI response HCC patients (figure 1A). Gene Ontology and Kyoto Encyclopedia of Genomes (KEGG) analyses revealed that metabolism and immunity-related terms were significantly enriched (online supplemental figure 1B,C). WWOX was detected in the serum of patients receiving PD-1 antibody treatment using ELISA and was more abundant in the responder group (figure 1B, online supplemental table 2). Representative MRIs are shown in figure 1C. In addition, WWOX protein expression was examined in different PD-1-responsive HCC tissues, and the IHC results suggested that WWOX was significantly upregulated in immune-responsive HCC tissues (figure 1D). Patients were divided into two groups based on the serum levels of WWOX in patients treated with PD-1. K-M analysis showed that low levels of WWOX in serum were associated with poor OS (27.59 vs 43.08 months) and recurrence-free survival (RFS, 23.97 vs 39.70 months) (figure 1E). To further clarify whether WWOX was required to mediate PD-1 resistance in HCC, we constructed a $WWOX^{low}$ humanized orthotopic HCC mouse model and compared PD-1 treatment responses. The results revealed that PD-1 treatment significantly reduced tumor growth in mice in the control but not the huh7-shWWOX group (figure 1F,G). Also, IHC results suggested that $CD8^{+}$ T-cell infiltration was reduced in Huh7-shWWOX tumors (figure 1H). These results

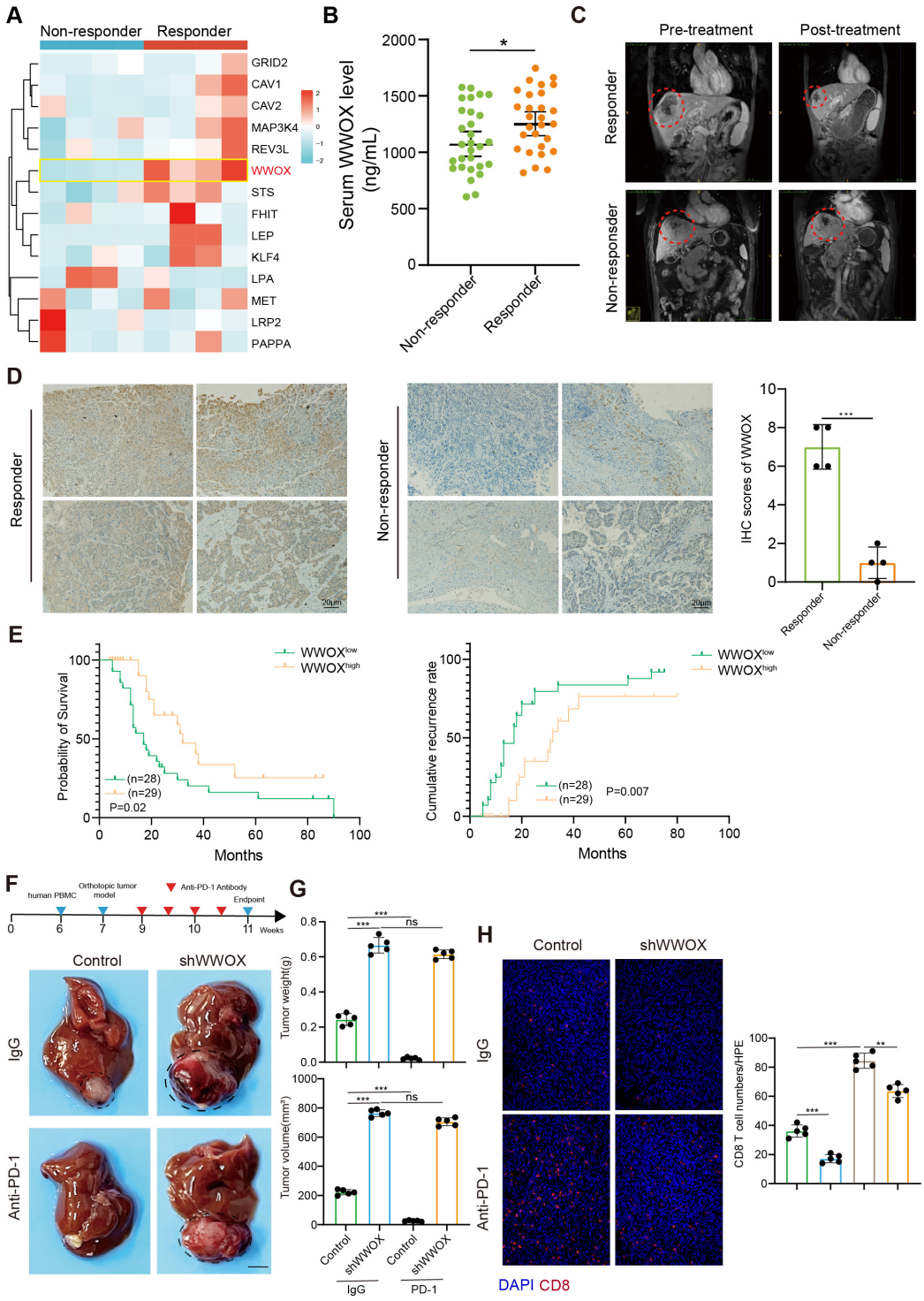

Figure 1 WWOX mediates the resistance of HCC to anti-PD-1 treatment. (A) Heatmap of differentially expressed CFSs genes in HCC patients who were ICI responders (n=4) and non-responders (n=4). (B) ELISA of WWOX levels in the serum of ICI responder (n=28) and non-responder (n=29) HCC patients. (C) Representative abdominal MRIs of HCC patients who were ICI responders and non-responders. (D) Representative IHC staining images of WWOX in HCC tissues from the indicated patients. Scale bar, 100 µm. (E) Kaplan-Meier survival curves showing the differences in overall survival (left) and cumulative recurrence rates (right) between high-WWOX and low-WWOX level in our cohort. (F) (Top): Schematic diagram of the orthotopic HCC tumor constructs in humanized mice and the schedule of anti-PD-1 antibody treatment of $WWOX^{low}$ tumors in humanized mice. (Bottom): Gross appearance of orthotopic HCC tumors in humanized mice in the indicated groups; (G) Weight and volume of orthotopic HCC tumors at the endpoint in the indicated groups. (H) (Left): Representative IF staining images of CD8 in HCC tumor tissues from the indicated group. Scale bar, 100 µm. (Right) Statistical analysis of the number of $CD8^+$ T cells in the indicated groups. *p<0.05, **p<0.01, ***p<0.001; Student's t-test. CFS, common fragile sites; HCC, hepatocellular carcinoma; ICI, immune checkpoint inhibitor; IF, immunofluorescent; TIME, tumor immune microenvironment; t-SNE, t-distributed stochastic neighbor embedding; WWOX, WW domain-containing oxidoreductase.

suggest that WWOX deficiency renders HCC resistant to PD-1 treatment.

WWOX deficiency is associated with suppressive TIME

To further observe the relationship between WWOX alterations and the TIME, we evaluated eight HCC tissues using cytometry by time-of-flight (CyTOF) analysis. Eight HCC tissues were divided into two groups according to the protein level of WWOX ($WWOX^{high}$ and $WWOX^{low}$, online supplemental figure 1D). Immune cells were clustered into 32 cell clusters based on the expression of 41 cell markers (figure 2A). Among these cells, macrophage infiltration was increased in the $WWOX^{low}$ subgroup, but no significant difference was observed in the infiltration of other immune cells (figure 2B,C). $CD8^+$ T subgroup analysis showed increased infiltration of the C14 subgroup in the $WWOX^{high}$ subgroup (online supplemental figure 1E). We further compared differences in macrophage and $CD8^+$ T-cell-related marker levels between the two groups. The results showed that M2 macrophage markers, such as CD68 and CD204, were elevated in the $WWOX^{low}$ subgroup, and $CD8^+$ T-cell-associated markers, such as PD-L1, Granzyme B and PD-1, were not different (figure 2D,E, online supplemental figure 1F). To further validate the above results of the effect of WWOX on the immune microenvironment, we performed multiple immunofluorescence staining of HCC tissues from eight cases treated with PD-1. The results revealed that WWOX was highly expressed in PD-1-responsive patients and was associated with high CD8 T cells and low macrophage infiltration (figure 2F). These results suggested that WWOX deficiency induced an immunosuppressive tumor microenvironment and attenuated the response to ICIs.

WWOX deficiency induces macrophage recruitment and immunosuppressive macrophage polarization

We constructed lentiviral stably transfected cell lines based on WWOX protein and mRNA levels in HCC cells (figure 3A, online supplemental figure 2A–C). To further examine whether WWOX is valuable for macrophage polarization and recruitment, we constructed an HCC and macrophage co-culture system (figure 3B). Co-culture with $WWOX^{low}$ HCC cells (HCCLM3-Vector and Huh7-shWWOX) upregulated CD163, MRC1, ARG-1, IL-10, and TGF-β mRNA levels and upregulated CD206 protein levels in macrophages (figure 3C,D). Chemotaxis assays showed that $WWOX^{low}$ HCC cells promoted macrophage recruitment (figure 3E). Similar results were found in PLC/PRF/5 and MHCC97H cells (online supplemental figure 2D–F). To further elucidate whether macrophage M2 polarization mediates WWOX-induced PD-1 resistance, we used Clophosome to clear macrophages in mice. Remarkably, PD-1 treatment significantly reduced tumor growth in the huh7-shWWOX group of mice after macrophage clearance compared with the control group (figure 3F,G).

To further determine whether the effect of WWOX on macrophage polarization affected the clinical prognosis of HCC patients, we performed IHC staining of tissues from 176 HCC patients. IHC staining revealed that WWOX expression negatively correlated with CD68 and CD206 expression (figure 3H, online supplemental table 3). Prognostic analysis revealed that HCC patients with $WWOX^{low}CD68^{high}$ and $WWOX^{low}CD206^{high}$ tumors had the worst OS, and $WWOX^{low}CD206^{high}$ was an independent prognostic factor (figure 3H, online supplemental table 4). These results suggest that WWOX deficiency induces macrophage M2-like reprogramming and mediates ICIs resistance.

OA-derived tumor tissue from patients with WWOX deficiency promotes immunosuppressive macrophage polarization

WWOX is closely associated with tumor metabolism, and we analyzed metabolites in the supernatants of HCC cells from control and shWWOX groups using untargeted metabolomics to further elucidate the molecular mechanisms of the effects of WWOX on macrophages (figure 4A). The results of difference analysis suggested that OA was most significantly upregulated in the supernatants of HCC cells in the shWWOX group compared with the control group (figure 4B). ELISAs further confirmed that the OA concentration was elevated in the supernatants of the $WWOX^{low}$ HCC cells compared with the control group (figure 4C, online supplemental figure 3B). Stimulation of PMA-treated THP-1 cells with OA significantly increased macrophage CD206 protein expression and M2-like macrophage marker mRNA levels (figure 4D). The transcriptomics results suggested that OA promoted M2 macrophage polarization via the mTOR signaling pathway (online supplemental figure 3A). Therefore, we hypothesized that WWOX affected macrophage polarization via OA.

To examine the biological mechanisms of the effects of WWOX on OA, we detected key enzymes of OA metabolism, SCD1 and SCD5. Western blot assays and qPCR confirmed that WWOX deficiency upregulated SCD5 protein and mRNA levels without affecting SCD1 (figure 4E, online supplemental figure 3C–E). To determine whether upregulated SCD5 was associated with increased OA, we used lentiviral shSCD5-transfected Huh7-shWWOX cells and lentiviral SCD5-transfected HCCLM3-WWOX cells and found these cells significantly attenuated the promotion of WWOX deficiency-induced OA synthesis (online supplemental figure 3F–H). Therefore, we hypothesized that SCD5 was a key mediator of the effects of WWOX on OA synthesis. To further clarify whether the SCD5-OA axis mediated the effects of WWOX on macrophages, we performed rescue experiments. Notably, SCD5 knockdown reversed the WWOX deficiency-induced increase in CD206 protein expression in macrophages (figure 4F). These results suggest that WWOX deficiency promotes M2 macrophage polarization primarily via transcriptional activation of the SCD5-OA axis.

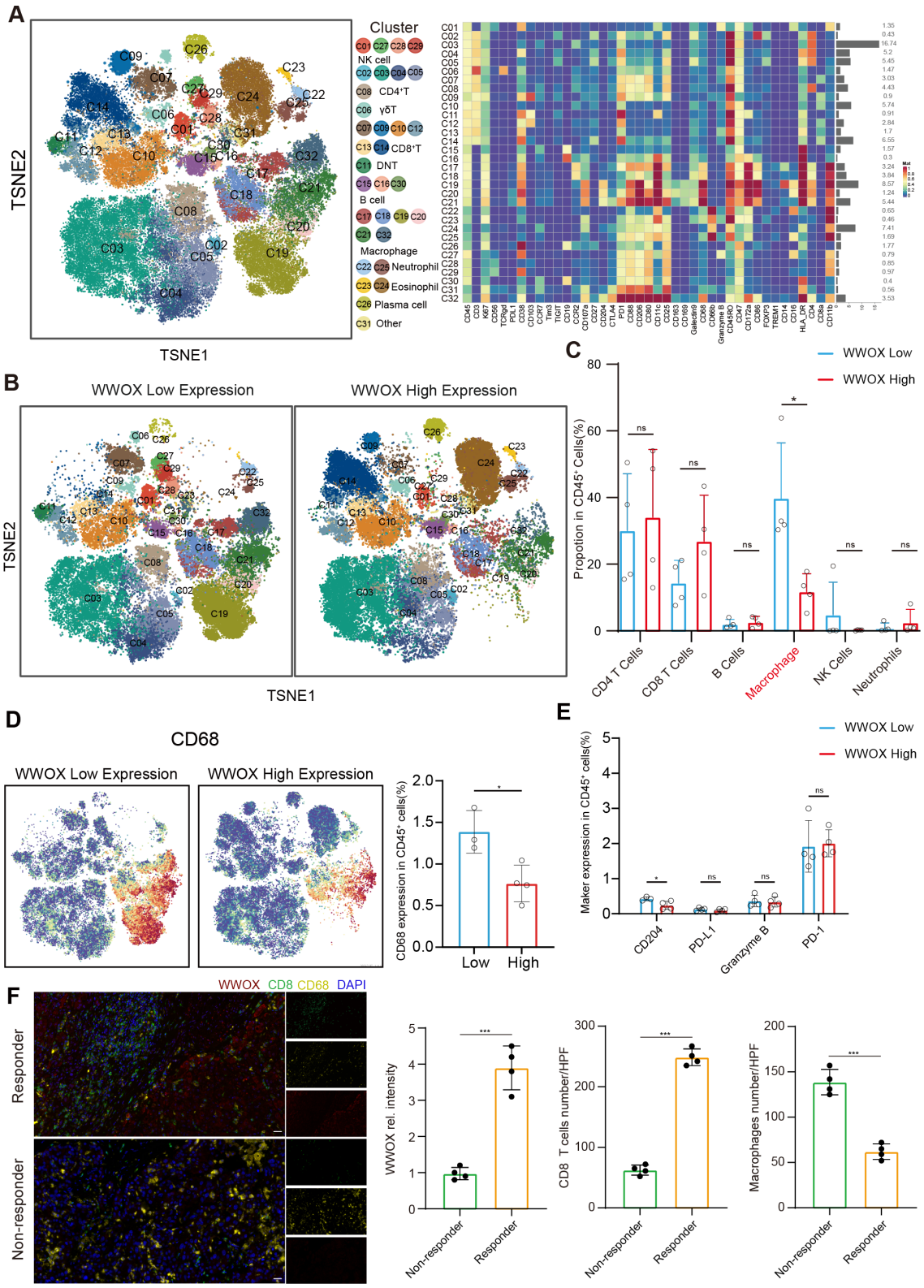

Figure 2 WWOX deficiency is associated with suppressive TIME. (A) (Left) t-SNE analysis of CyTOF data of immune cells in eight HCC tissues. (Right) Heatmap of the expression of 41 markers in all 32 subclusters. (B) t-SNE plots of immune cells in HCC tissues from the WWOX high/low subgroup. (C) Proportion of tumor-infiltrating immune cells in HCC tissues from the two groups. (D) (Left) t-SNE plots of CD68 expression levels in the indicated groups. (Right) CD68 expression levels in immune cells in both groups. (E) Expression of CD204, PD-L1, Granzyme B and PD-1 in $CD45^+$ cells in the indicated groups. (F) (Left): The representative image of HCC tissue stained with WWOX (red), CD8 (green), CD68 (yellow). (Right): Statistical analysis of the number of $CD8^+$ T cells, macrophages and WWOX expression in the indicated groups. *p<0.05, ***p<0.001; Student's t-test. CyTOF, cytometry by time-of-flight; HCC, hepatocellular carcinoma; TIME, tumor immune microenvironment; t-SNE, t-distributed stochastic neighbor embedding; WWOX, WW domain-containing oxidoreductase.

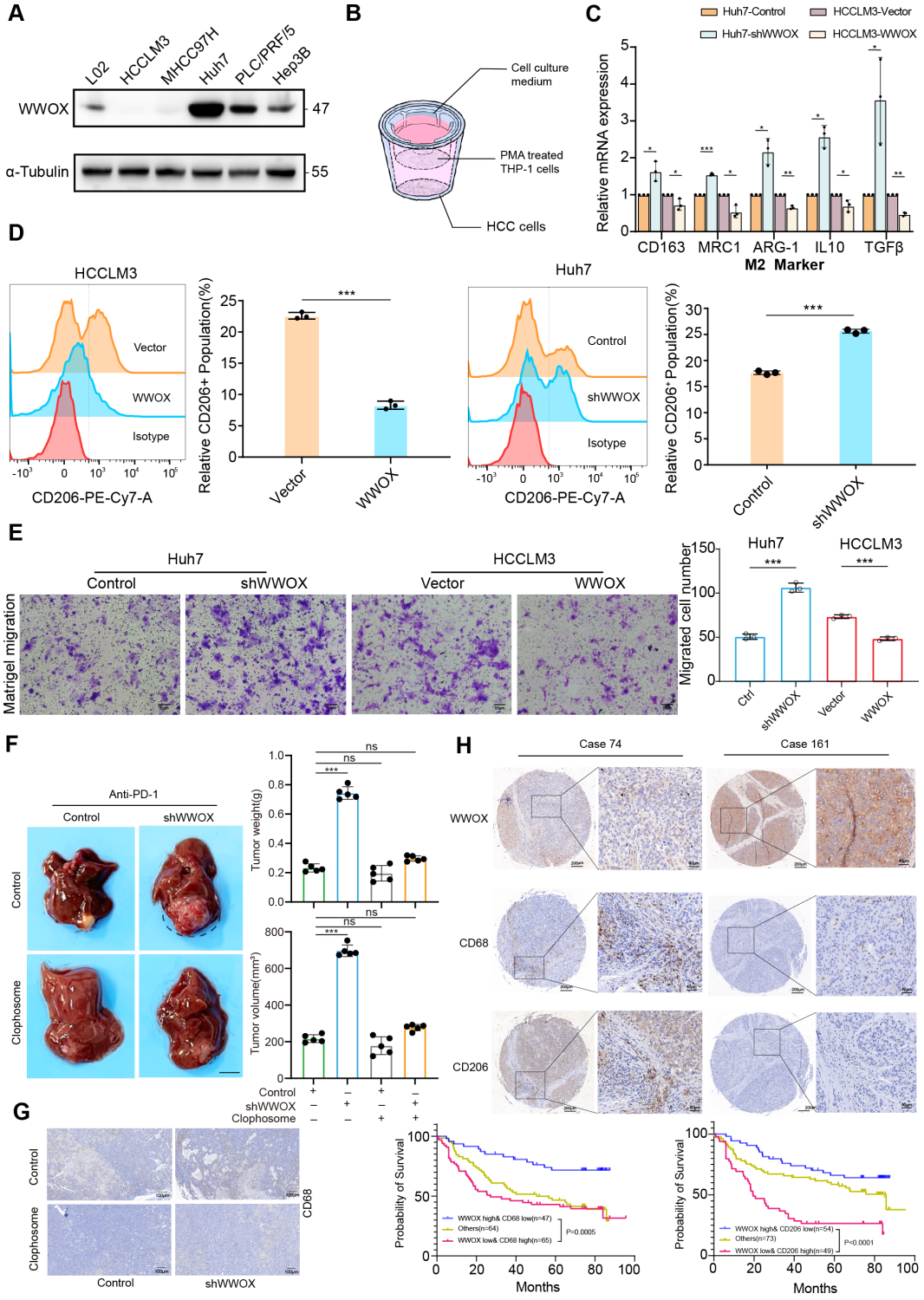

Figure 3 WWOX deficiency induces macrophage recruitment and immunosuppressive macrophage polarization. (A) Western blot analysis of WWOX levels in HCC cells. (B) Schematic diagram of HCC cells and macrophages (PMA-treated) co-cultured in vitro. (C) qPCR analysis of the mRNA levels of CD163, MRC1, ARG1, IL-10 and TGF-β in macrophages (PMA-treated) after co-culture with HCC cells. (D) Flow cytometry analysis of CD206 expression on the surface of macrophages (PMA-treated) after co-culture with HCC cells. (E) Chemotaxis assays were used to analyze the effect of Huh7-shWWOX and MHCCLM3-WWOX cell supernatants on macrophage (PMA-treated) migration. Scale bar, 50 µm. (F) (Left) Gross appearance of orthotopic HCC tumors with anti-PD-1 treatment in humanized mice in the indicated groups; (Right) Weight and volume of orthotopic HCC tumors at the endpoint in the indicated groups. (G): Representative IHC images of CD68 in HCC tumors of indicated groups. (H) (Top) Representative IHC images of WWOX, CD68 and CD206 in HCC tissues. Scale bar, 200 µm (left) and 50 µm (right). (Bottom) Kaplan-Meier survival curves for patients stratified according to WWOX/CD68 and WWOX/CD206 expression. *p<0.05, **p<0.01, ***p<0.001; Student's t-test and log-rank test. HCC, hepatocellular carcinoma; IHC, immunohistochemistry; PMA, phorbol-12-myristate-13-acetate; qPCR, quantitative real-time PCR; WWOX, WW domain-containing oxidoreductase.

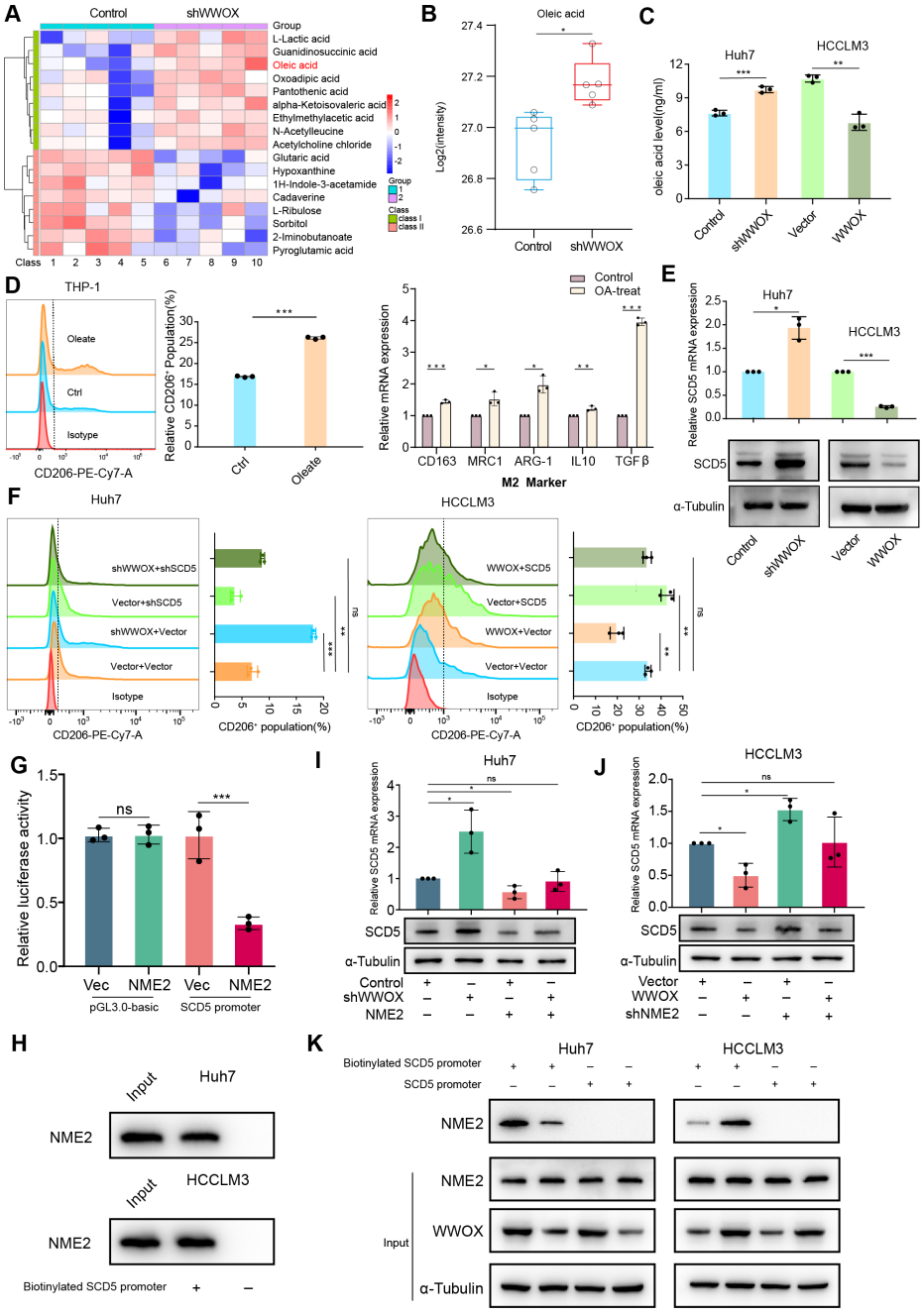

Figure 4 NME2/SCD5 axis-mediated release of oleic acid from HCC cells promotes immunosuppressive macrophage polarization. (A) Untargeted metabolic analysis of the control and shWWOX groups of Huh7 cell supernatants. Groups 1 and 2 represent WWOX knockdown and control HCC cells, respectively. Classes I and II represent upregulated and downregulated metabolites. (B) Differential analysis of OA content in supernatants of WWOX knockdown and control HCC cells. (C) ELISA was used to analyze the OA concentration in the supernatants of the indicated HCC cells. (D) (Left) Flow cytometry analysis of CD206 expression on the surface of macrophages after OA treatment. (Right) qPCR analysis of the mRNA levels of M2 markers in macrophages after OA treatment. (E) Western blot and qPCR analyses of the protein and mRNA levels of SCD5 in the indicated HCC cells. (F) (Left) Flow cytometry analysis of CD206 levels in macrophages co-cultured with Huh7-shWWOX cells transfected with lentivirus-shSCD5. (Right) Flow cytometry analysis of CD206 levels in macrophages after co-culture with MHCCLM3-shWWOX cells transfected with lentivirus-SCD5. (G) The function of NME2 in suppressing SCD5 transcription was analyzed using dual luciferase assay in the SCD5 promoter region. (H) DNA pulldown assay of NME2 binding to the SCD5 promoter in the indicated HCC cells. (I) Western blot and qPCR analyses of the mRNA and protein levels of SCD5 after lentiviral NME2-mediated transfection of Huh7-shWWOX cells; (J) Western blot and qPCR analyses of the mRNA and protein levels of SCD5 after lentiviral shNME2-mediated transfection of HCCLM3-SWWOX cells. (K) A DNA pulldown assay was used to analyze the effect of WWOX on the binding affinity of NME2 to the SCD5 promoter in the indicated HCC cells. *p<0.05, **p<0.01, ***p<0.001; Student's t-test or one-way ANOVA with a post hoc Least Significant Difference (LSD) test. ANOVA, analysis of variance; HCC, hepatocellular carcinoma; OA, oleic acid; WWOX, WW domain-containing oxidoreductase; qPCR, quantitative real-time PCR.

NME2 is a transcription factor for SCD5 that promotes immunosuppressive macrophage polarization

Because WWOX deficiency transcriptionally activates SCD5, we further screened for potential transcription factors related to SCD5. The direct binding of WWOX to transcription factors was reported in previous studies.[23] Therefore, we detected SCD5 promoter-binding proteins and WWOX direct-binding proteins using liquid chromatography-tandem mass spectrometry (LC-MS/MS) and obtained four proteins using intersection analysis of the results with the transcription factor database (Cistrome, AnimalTFDB) (online supplemental figure 4A). Among these factors, overexpression of NME2 had the most significant effect on the SCD5 protein level (online supplemental figure 4B,C). Western blot assays showed that WWOX did not affect NME2 protein levels (online supplemental figure 4D). To determine whether NME2 was a transcription factor, we constructed a dual-luciferase reporter plasmid containing the SCD5 promoter region. Notably, NME2 significantly reduced SCD5 luciferase activity (figure 4G). A DNA pull-down assay using the SCD5-specific promoter confirmed that NME2 bound to the SCD5 promoter (figure 4H). These results indicate that NME2 binds to the SCD5 promoter region, which suggests that NME2 is a transcriptional repressor of SCD5.

To determine whether NME2 mediates WWOX deficiency-induced macrophage M2 polarization, we transfected Huh7-shWWOX cells with lentiviral NME2 and HCCLM3-WWOX cells with lentiviral shNME2 (online supplemental figure 4E). These cells significantly attenuated the promotion of SCD5 activation and WWOX deficiency-induced OA synthesis and reduced macrophage CD206 protein expression (figure 4I,J, online supplemental figure 4F,G). These findings suggest that the WWOX-NME2-SCD5 axis is involved in regulating M2 macrophage polarization.

To elucidate the intrinsic mechanism of the effects of WWOX on NME2 regulation of SCD5 transcription, we performed nuclear-cytoplasmic extraction experiments. The results revealed that WWOX did not affect the protein localization of NME2 (online supplemental figure 4H). Previous studies found that the binding of transcription factors to target gene promoters affected their transcriptional activity.[24] We hypothesized that WWOX affected NME2 binding to the SCD5 promoter. By constructing an SCD5-specific promoter, a DNA pull-down assay showed that NME2 binding to the SCD5 promoter was reduced in Huh7-shWWOX cells, and overexpression of WWOX in HCCLM3 cells promoted NME2 binding to the SCD5 promoter (figure 4K). These results suggest that WWOX inhibits SCD5 transcription by promoting the binding of NME2 to the SCD5 promoter.

WWOX competes with KAT1 for binding to NME2 to inhibit the acetylation of NME2 at site 31 mediated by KAT1

To further investigate the specific mechanism of WWOX promotion of NME2 binding to the SCD5 promoter, we determined the direct interaction between WWOX and NME2 based on the results of LC-MS/MS. Immunoprecipitation and immunofluorescence analyses demonstrated the interaction and co-localization of WWOX with NME2 in HCC cells (figure 5A,B). We mapped the structural domains involved in the interaction between WWOX and NME2 and found that the WWOX (106-414) and NME2 (67-152) domains were necessary for their interaction (figure 5C).

Post-translational modifications of transcription factors have important effects on transcription factor function.[24 25] Acetylation modifications affect the binding of transcription factors to target gene promoters, and the presence of acetylation modifications has been reported for other family members of nucleoside diphosphate kinase.[24 26] Therefore, we hypothesized that WWOX regulated the acetylation of NME2 and affected its binding to the SCD5 promoter. Notably, Western blot assays showed that the acetylation level of NME2 was elevated in Huh7-shWWOX cells, and the acetylation level of NME2 was reduced in HCCLM3-WWOX cells compared with their counterparts (figure 5D). This finding suggested that WWOX affected the acetylation of NME2. We used mass spectrometry to identify the major acetylation sites of NME2. The result showed that NME2 was primarily acetylated at lysine residues 31, and this site is highly conserved in different species (figure 5E, online supplemental figure 5A). To further confirm the acetylation site of NME2, we prepared lysine-to-arginine mutant NME2-K31R plasmids and transfected it into Huh7 cells. As shown in figure 5F, NME2 acetylation was significantly reduced in cells transfected with the NME2-K31R mutation.

To further identify the acetyltransferase responsible for NME2 acetylation, we used a mass spectrometry approach and found that KAT1 may be a candidate acetyltransferase for NME2 (online supplemental figure 5B). Further immunoprecipitation analysis demonstrated the interaction of endogenous and exogenous NME2 with KAT1 (online supplemental figure 5C). To demonstrate that KAT1 affects the acetylation of NME2, we cotransfected Huh7 cells with His-tagged NME2 and Flag-tagged KAT1 and found that KAT1 significantly increased the acetylation level of NME2 (figure 5G). Cotransfection with the shKAT1 plasmid significantly reduced the level of NME2 acetylation in NME2 WT-transfected cells, which was fully restored in NME2-K31Q-mutated cells (figure 5G). We investigated whether KAT1 mediated the WWOX-induced differences in NME2 acetylation. Transfection of the KAT1 and shKAT1 plasmids into Huh7-shWWOX and HCCLM3-WWOX cells, respectively, revealed that KAT1 completely restored the WWOX-induced differences in NME2 acetylation (online supplemental figure 5D). Further immunoprecipitation analysis revealed that transfection of WWOX reduced the binding capacity of NME2 to KAT1 (figure 5H). Therefore, KAT1 is an acetyltransferase of NME2 and is involved in the WWOX-induced reduction in NME2 acetylation at site 31. We next explored the interaction patterns of WWOX, NME2, and

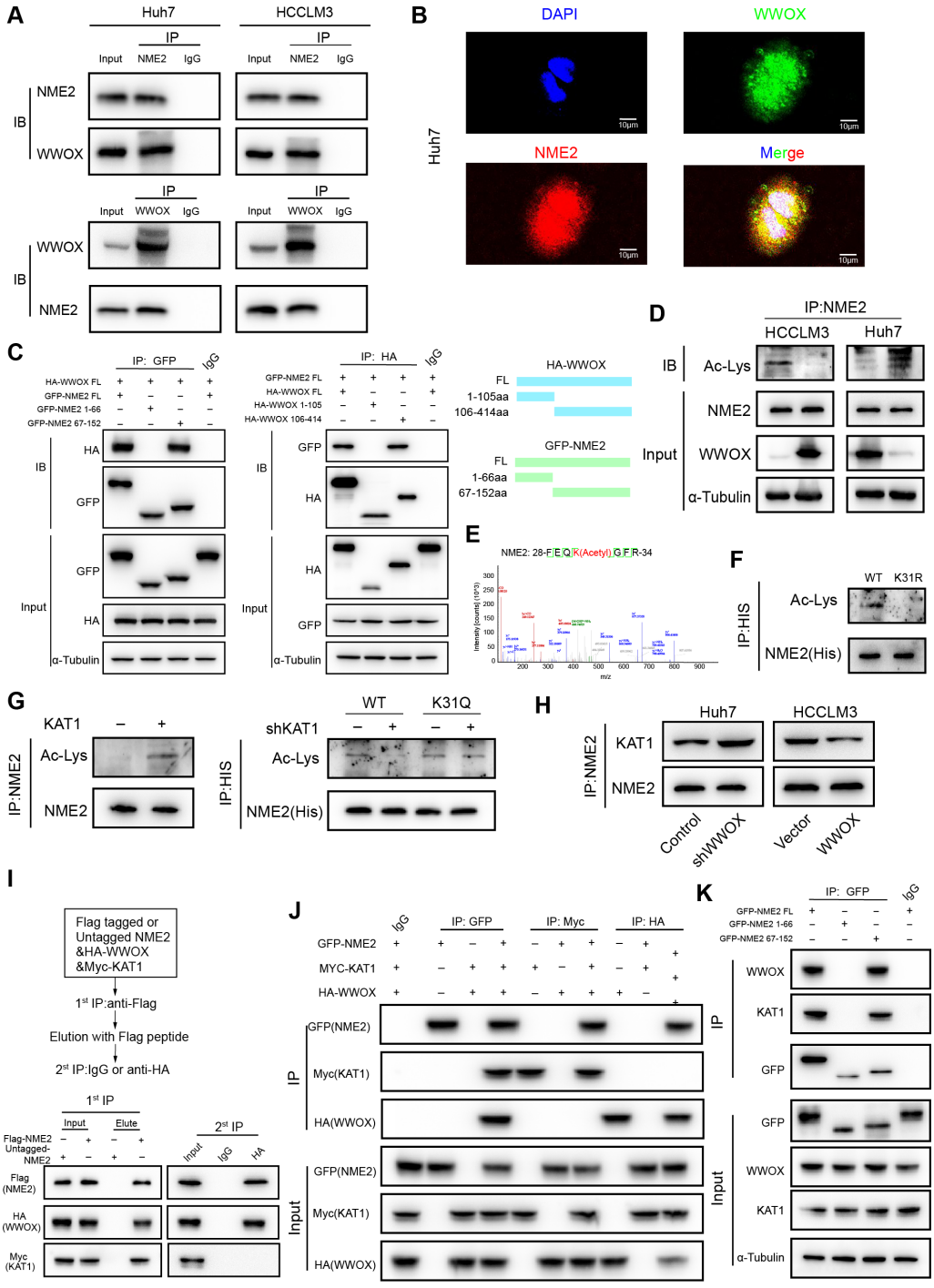

Figure 5 WWOX binds NME2 in a competitive manner with KAT1 to inhibit the acetylation of NME2 at site 31 mediated by KAT1. (A, B) Co-IP and IF experiments showed the interaction and co-localization of WWOX and NME2 in HCC cells. Scale bar, 10 μm. (C) (Left) HA-WWOX FL or fragments were cotransfected with GFP-NME2 FL or fragments in 293T cells, and Western blot detection of mutually interacting structural domains was performed; (Right): Schematic representation of the structural domains of WWOX and NME2. (D) Western blot analysis of NME2 acetylation levels in the indicated HCC cells. (E) Mass spectrometry was used to identify possible acetylation sites in NME2. (F) Huh7 cells were transfected with His-NME2 WT, His-NME2 K31R site mutant plasmids, and NME2 acetylation was detected via Co-IP. (G) Huh7 cells were cotransfected with the above plasmids, and the level of NME2 acetylation was detected using a Co-IP assay. (H) Co-IP assay was used to detect the amount of NME2 bound to KAT1 in the indicated HCC cells. (I, M) Top: Schematic showing the flow of sequential IP assays. Bottom: IP analyses showed interactions of NME2 with WWOX/KAT1 but no binding of WWOX to KAT1. (J) IP analyses of cell lysates from HEK293T cells transfected with GFP-NME2, Myc-KAT1, and HA-WWOX using the indicated tag antibodies. (K) IP analyses of cell lysates from HEK293T cells transfected with GFP-NME2 FL or fragments using the indicated tag antibodies. HCC, hepatocellular carcinoma; IF, immunofluorescence; IP, immunoprecipitation; KAT1, histone acetyltransferase 1; NME2, nucleoside diphosphate kinase 2; qPCR, quantitative real-time PCR; SCD5, stearoyl-CoA desaturase 5; WWOX, WW domain-containing oxidoreductase.

KAT1. Sequential IP assays showed that NME2 that bound WWOX was unable to rebind KAT1, which was validated in further Co-IP assays, suggesting that WWOX interacts with NME2 in a mutually exclusive manner with KAT1 (figure 5I,J). To further clarify the structural domain of NME2-WWOX/KAT1 binding, NME2 full-length and fragments were used to perform IP experiments. Our results indicated that both WWOX and KAT1 bind to the Nucleoside diphosphate kinase (67-152aa) domain of NME2 (figure 5K). Hence, WWOX interacts competitively with KAT1 to NME2 to suppress NME2 acetylation.

We investigated whether NME2 acetylation mediated the WWOX-mediated suppression of SCD5 transcription. The results of DNA pulldown experiments showed complete restoration of NME2 binding to the SCD5 gene promoter in KAT1-transfected HCCLM3-WWOX cells and shKAT1-transfected Huh7-shWWOX cells compared with controls (online supplemental figure 5E). The mRNA and protein levels of SCD5 were similarly fully restored in the transfected NME2-K31R group compared with the NME2 WT group (online supplemental figure 5F,G). These results suggest that NME2 acetylation attenuates the ability of NME2 to bind to the SCD5 gene promoter and mediates WWOX-mediated suppression of SCD5 transcription.

Pharmacological blockade of SCD5 signaling enhances the therapeutic effect of anti-PD-1 therapy in humanized WWOX^{low} tumor-bearing mice

We further examined whether blockade of SCD5 signaling improved the efficacy of anti-PD-1 therapy. A humanized orthotopic HCC mouse model was constructed with Huh7 cells, which was administered anti-PD-1 antibody, SCD1/5-IN-1 2 weeks later (figure 6A). The results revealed that blockade of SCD5 signaling in combination with anti-PD-1 treatment inhibited tumor growth and lung metastasis more than the control treatment or single treatment alone, and no difference in liver function was observed (figure 6B–D, online supplemental figure 6A–C). IHC analysis of the combination group revealed that M2 macrophage infiltration was reduced in tumor tissues (figure 6E, online supplemental figure 2D–G). These results suggest that WWOX deficiency promotes HCC growth and increases M2 macrophage infiltration in humanized mice and further blockade of SCD5 signaling improved the efficacy of anti-PD-1 therapy.

Correlation and clinical prognostic value of WWOX/NME2/SCD5 axis in patients with HCC

To verify the correlation and prognostic value of WWOX, NME2 and SCD5, we performed IHC staining using tissue microarrays (figure 7A). Correlation analyses suggested that WWOX negatively correlated with SCD5 expression but not with NME2 expression (figure 7B). Notably, survival analysis revealed that patients with WWOX^{low}/SCD5^{high} HCC had the shortest OS (figure 7C). In addition, HCC patients with SCD5^{high} and NME2^{low} tumors had poorer OS (figure 7D,E). These results emphasize the important prognostic value of the WWOX/NME2/SCD5 axis in HCC patients.

DISCUSSION

ICI therapy has become an effective treatment for solid tumors. However, only some patients achieve therapeutic benefits due to clinical tolerance in HCC patients. The present study indicated that WWOX deficiency was related to poor prognosis and poor treatment response to ICIs. Specifically, we found that WWOX deficiency promoted acetylation of NME2 at site 31 via KAT1, which inhibited its binding to the SCD5 promoter region. This process promotes increased OA secretion from tumor cells and macrophage M2 polarization, which induces HCC immune escape. Therefore, the present study reveals the molecular mechanism of WWOX deficiency promotion of HCC immune escape, which is valuable for improving the understanding of ICI tolerance and guiding clinical therapy.

CFSs and associated genes are frequently deleted or rearranged in many tumor cells and are associated with tumor genomic instability.[17] At present, the reason for the loss of WWOX expression in tumors remains unclear. Studies have shown that WWOX expression downregulation is observed in a variety of tumors, including HCC, and this result may be related to exposure to carcinogens, which can cause fragile site break, homozygous loss or heterozygous loss.[27] The role of point and somatic mutations in WWOX loss was not observed. In addition, mechanisms such as epigenetic (methylation) and post-translational modification (ubiquitination) have also been shown to regulate WWOX expression.[28 29] Therefore, the mechanism of WWOX deficiency in tumors is multifaceted and still needs to be further explored. Several studies showed that WWOX deficiency accelerated tumor progression, and it was closely related to tumor metabolism.[19 30] WWOX/HIFA axis is involved in the regulation of glucose metabolism and can also change the high density lipoprotein and lipoprotein metabolism, which plays an important role in a variety of diseases, including tumors.[30 31] However, the relationships between WWOX and the immune microenvironment and response to immunotherapy have rarely been reported. The present study used high-throughput transcriptomics and CyTOF analysis of clinical samples and determined that WWOX deficiency was significantly associated with the ICIs treatment response and induced M2 macrophage polarization, which resulted in an immunosuppressive microenvironment. We further determined the effect of WWOX on the immune microenvironment and its value in predicting the response to immunotherapy using ELISA to detect WWOX levels in the serum of HCC patients and humanized mice. In conclusion, these results enrich our understanding of the role of WWOX in tumor immunity and provide a basis for its potential use as a clinical marker for predicting the efficacy of immunotherapy.

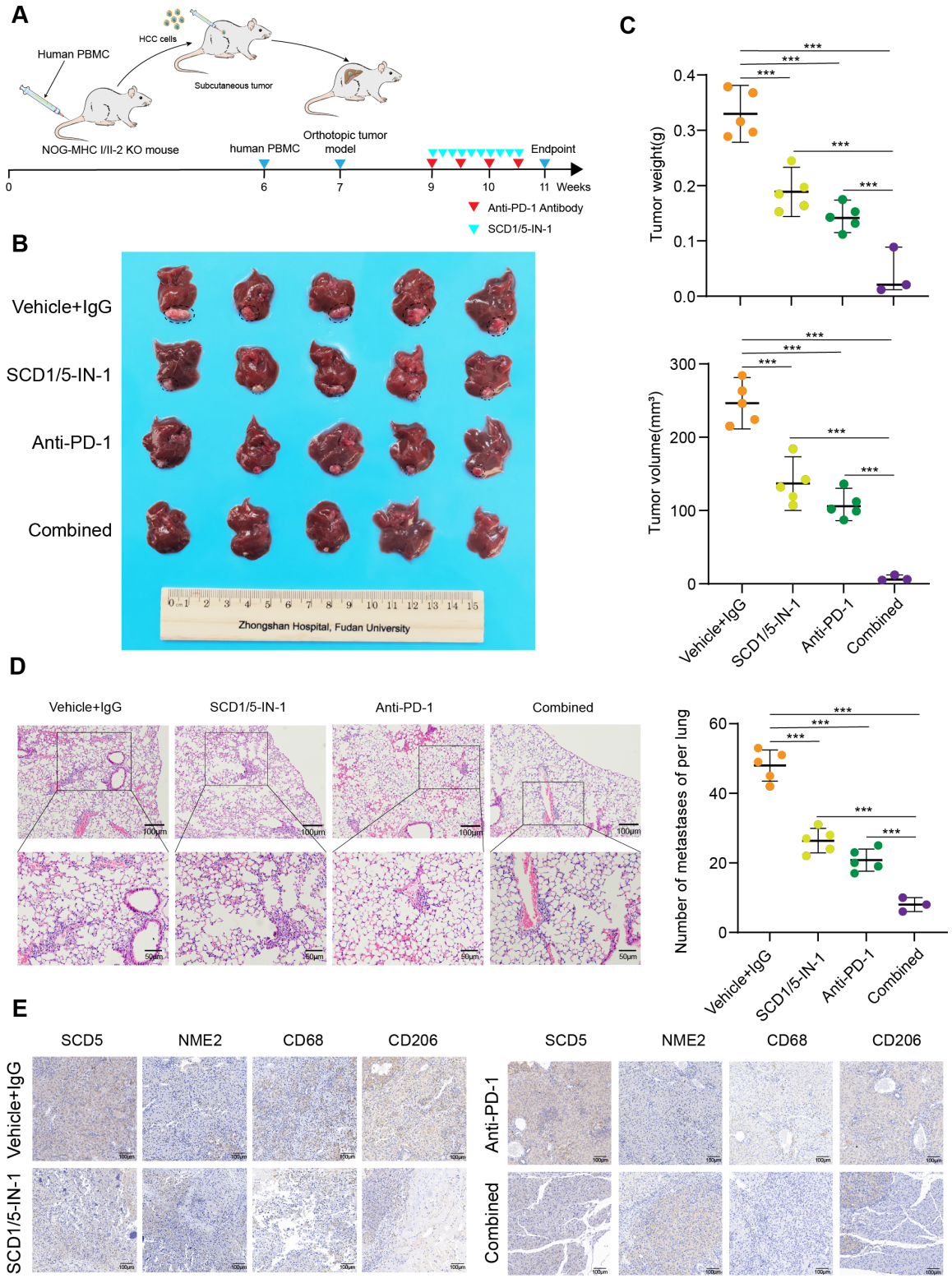

Figure 6 Pharmacological blockade of SCD5 signaling enhances the therapeutic effect of anti-PD-1 therapy in humanized WWOX^{low} tumor-bearing mice. (A) Schematic diagram of the orthotopic HCC tumor constructs in humanized mice and the schedule of anti-PD-1 antibody and SCD1/5-IN-1 treatment of WWOX^{low} tumors in humanized mice. (B) Gross appearance of orthotopic HCC tumors in humanized mice in the indicated groups; (C) Weight and volume of orthotopic HCC tumors at the endpoint in the indicated groups. (D) Representative images of HE-stained mouse lungs from the indicated groups (left) and differential analysis of the number of metastases per lung (right). Scale bar, 100 µm (top) and 50 µm (bottom). (E) Representative IHC staining images of CD68, CD206, NME2 and SCD5 in orthotopic HCC tumor tissues from the indicated groups. Scale bar, 100 µm. ***p<0.001; one-way ANOVA with a post hoc LSD test. ANOVA, analysis of variance; HCC, hepatocellular carcinoma; IHC, immunohistochemistry; NME2, nucleoside diphosphate kinase 2; SCD5, stearoyl-CoA desaturase 5; WWOX, WW domain-containing oxidoreductase.

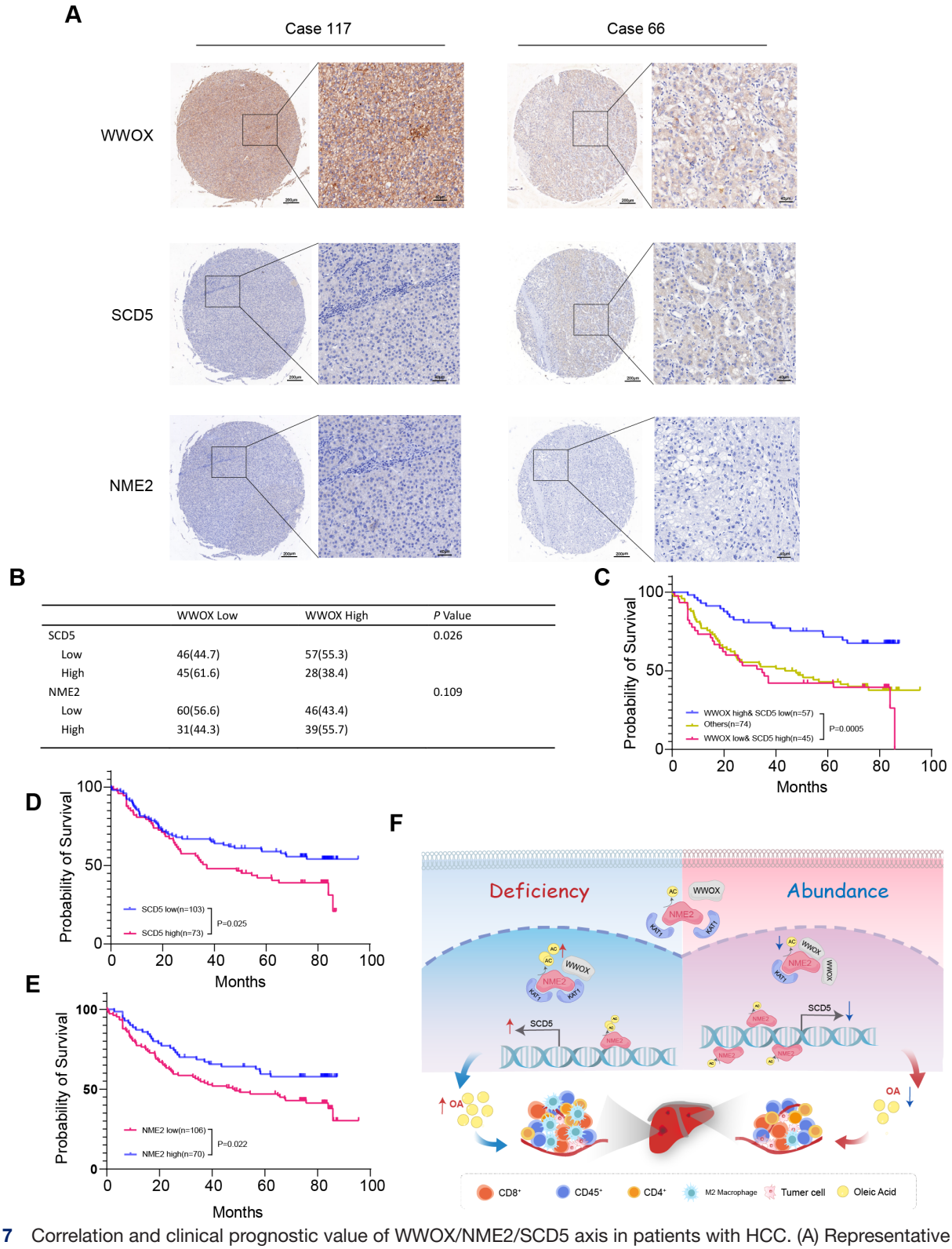

B

	WWOX Low	WWOX High	*P* Value
SCD5			0.026
Low	46(44.7)	57(55.3)	
High	45(61.6)	28(38.4)	
NME2			0.109
Low	60(56.6)	46(43.4)	
High	31(44.3)	39(55.7)	

Figure 7 Correlation and clinical prognostic value of WWOX/NME2/SCD5 axis in patients with HCC. (A) Representative images of IHC staining of WWOX, SCD5 and NME2 in HCC tissues. Scale bar, 200 µm (Left) and 40 µm (Right). (B) Correlation analysis of WWOX with SCD5 and NME2 expression. (C) Kaplan-Meier curve analysis of WWOX/SCD5 expression and HCC prognosis. (D) Kaplan-Meier curve analysis of SCD5 expression with HCC prognosis. (E) Kaplan-Meier curve analysis of NME2 expression and HCC prognosis. (F) Schematic illustration of the role of WWOX in regulating the immune microenvironment in HCC. WWOX inhibited the synthesis of oleic acid in HCC cells and immunosuppressive polarization in macrophages by competitively binding KAT1 to NME2, which inhibited the acetylation of NME2 at site 31 and promoted the binding of NME2 to the SCD5 promoter region. Blockade of SCD5 signaling enhances the therapeutic effect of anti-PD-1 therapy in HCC patients with low WWOX expression. $\chi 2$ test (log-rank test). HCC, hepatocellular carcinoma; IHC, immunohistochemistry; NME2, nucleoside diphosphate kinase 2; SCD5, stearoyl-Coa desaturase 5; WWOX, WW domain-containing oxidoreductase.

OA is an important product of fatty acid synthesis, and it promotes tumor development via multiple pathways.[32 33] OA induces the polarization of bone marrow-derived myeloid cells into an immunosuppressive phenotype via the mTOR pathway and promotes tumor development.[34] M2 macrophage polarization is important for inducing an immunosuppressive microenvironment, and it correlates with the ICI response.[35 36] Consistent with these findings, our results revealed that OA promoted M2 macrophage polarization, and transcriptomics revealed that OA activated the macrophage mTOR pathway. SCD5 is a key enzyme in OA production. However, the prognostic value and function of SCD5 in HCC have not been reported. This study demonstrated for the first time that high expression of SCD5 was associated with poor prognosis in HCC patients, and WWOX deficiency transcriptionally activated SCD5 and promoted increased OA synthesis. The nucleoside diphosphate kinase NME2 is a transcription factor for MYC, and it performs multiple biological functions.[37] The present study found that low expression of NME2 was associated with poor prognosis in HCC patients. However, the mechanism of post-translational modification of NME2 has not been determined. This study revealed that WWOX deficiency promoted the binding of KAT1 to NME2 and subsequently promoted its acetylation. Taken together, our results emphasize the value of NME2/SCD5/OA axis activation in the immune escape of HCC cells.

In conclusion, our study elucidated the mechanism by which the WWOX/NME2/SCD5/OA axis induced macrophage reprogramming and caused HCC immune escape. This study provides an important reference for the clinical application of WWOX as a predictive marker for the efficacy of ICI therapy and for targeting SCD5 to improve the sensitivity of HCC patients to ICI therapy.

Author affiliations
[1]Department of Liver Surgery and Transplantation, Liver Cancer Institute, Zhongshan Hospital, Fudan University, Key Laboratory of Carcinogenesis and Cancer Invasion, Ministry of Education, Shanghai, China
[2]Department of Hepatobiliary and Pancreatic Surgery, Minhang Hospital, Fudan University, Shanghai, China
[3]Biomedical Research Centre, Zhongshan Hospital, Fudan University, Shanghai, China
[4]Graduate Institute of Biomedical Sciences, Research Center for Cancer Biology and Center for Molecular Medicine, China Medical University, Taichung, Taiwan

Contributors SL, SY and MinX designed and performed experiments, analyzed data and wrote the manuscript. JW, ZH and MinghaoX analyzed clinical data. WX, YY and YS assisted in animal experiments. M-CH, NR and CZ supervised the entire project, designed the experiments and revised the manuscript. M-CH, NR and CZ has verified the underlying data. CZ is the guarantor.

Funding This study was supported by grants from the National Natural Science Foundation of China (82073208 and 82472804 to NR, 82103521 and 82472816 to CZ), Sino-German Mobility Program (M-0603 to NR), Shanghai Shen Kang Hospital Development Center New Frontier Technology Joint Project (SHDC12021109 to NR), Shanghai Sailing Program (21YF1407500 to CZ), and the China Postdoctoral Science Foundation (2021M690674 to CZ, 2023T160123 to CZ).

Competing interests None declared.

Patient consent for publication Consent obtained directly from patient(s).

Ethics approval This study involves human participants and was approved by the Clinical Research Ethics Committee of Zhongshan Hospital, Fudan University, ID: B-2021-143R. Participants gave informed consent to participate in the study before taking part.

Provenance and peer review Not commissioned; externally peer reviewed.

Data availability statement Data are available on reasonable request.

Supplemental material This content has been supplied by the author(s). It has not been vetted by BMJ Publishing Group Limited (BMJ) and may not have been peer-reviewed. Any opinions or recommendations discussed are solely those of the author(s) and are not endorsed by BMJ. BMJ disclaims all liability and responsibility arising from any reliance placed on the content. Where the content includes any translated material, BMJ does not warrant the accuracy and reliability of the translations (including but not limited to local regulations, clinical guidelines, terminology, drug names and drug dosages), and is not responsible for any error and/or omissions arising from translation and adaptation or otherwise.

Open access This is an open access article distributed in accordance with the Creative Commons Attribution Non Commercial (CC BY-NC 4.0) license, which permits others to distribute, remix, adapt, build upon this work non-commercially, and license their derivative works on different terms, provided the original work is properly cited, appropriate credit is given, any changes made indicated, and the use is non-commercial. See http://creativecommons.org/licenses/by-nc/4.0/.

ORCID iDs
Mien-Chie Hung http://orcid.org/0000-0003-4317-4740
Ning Ren http://orcid.org/0000-0001-9776-2471

REFERENCES

1 Zhang C-H, Cheng Y, Zhang S, *et al*. Changing epidemiology of hepatocellular carcinoma in Asia. *Liver Int* 2022;42:2029–41.
2 Petrick JL, McGlynn KA. The changing epidemiology of primary liver cancer. *Curr Epidemiol Rep* 2019;6:104–11.
3 Kulik L, El-Serag HB. Epidemiology and Management of Hepatocellular Carcinoma. *Gastroenterology* 2019;156:477–91.
4 Greten TF, Lai CW, Li G, *et al*. Targeted and Immune-Based Therapies for Hepatocellular Carcinoma. *Gastroenterology* 2019;156:510–24.
5 Villanueva A. Hepatocellular Carcinoma. *N Engl J Med* 2019;380:1450–62.
6 Vogel A, Saborowski A. Current strategies for the treatment of intermediate and advanced hepatocellular carcinoma. *Cancer Treat Rev* 2020;82:101946.
7 Wei SC, Duffy CR, Allison JP. Fundamental Mechanisms of Immune Checkpoint Blockade Therapy. *Cancer Discov* 2018;8:1069–86.
8 El-Khoueiry AB, Sangro B, Yau T, *et al*. Nivolumab in patients with advanced hepatocellular carcinoma (CheckMate 040): an open-label, non-comparative, phase 1/2 dose escalation and expansion trial. *Lancet* 2017;389:2492–502.
9 Zhu AX, Finn RS, Edeline J, *et al*. Pembrolizumab in patients with advanced hepatocellular carcinoma previously treated with sorafenib (KEYNOTE-224): a non-randomised, open-label phase 2 trial. *Lancet Oncol* 2018;19:940–52.
10 Schreiber RD, Old LJ, Smyth MJ. Cancer immunoediting: integrating immunity's roles in cancer suppression and promotion. *Science* 2011;331:1565–70.
11 Rabinovich GA, Gabrilovich D, Sotomayor EM. Immunosuppressive strategies that are mediated by tumor cells. *Annu Rev Immunol* 2007;25:267–96.
12 Sangro B, Sarobe P, Hervás-Stubbs S, *et al*. Advances in immunotherapy for hepatocellular carcinoma. *Nat Rev Gastroenterol Hepatol* 2021;18:525–43.
13 Zhang J, Zhang Q, Lou Y, *et al*. Hypoxia-inducible factor-1α/interleukin-1β signaling enhances hepatoma epithelial-mesenchymal transition through macrophages in a hypoxic-inflammatory microenvironment. *Hepatology* 2018;67:1872–89.
14 Li J, Xue J, Ling M, *et al*. MicroRNA-15b in extracellular vesicles from arsenite-treated macrophages promotes the progression of hepatocellular carcinomas by blocking the LATS1-mediated Hippo pathway. *Cancer Lett* 2021;497:137–53.
15 DeNardo DG, Ruffell B. Macrophages as regulators of tumour immunity and immunotherapy. *Nat Rev Immunol* 2019;19:369–82.
16 Li S, Wu X. Common fragile sites: protection and repair. *Cell Biosci* 2020;10:29.
17 Glover TW. Common fragile sites. *Cancer Lett* 2006;232:4–12.
18 Chen W, Zhou C, Zhang W, *et al*. Association of WWOX rs9926344 polymorphism with poor prognosis of hepatocellular carcinoma. *J Cancer* 2018;9:1239–47.

19 Yang T, Xu R, Huo J, *et al*. WWOX activation by toosendanin suppresses hepatocellular carcinoma metastasis through JAK2/Stat3 and Wnt/β-catenin signaling. *Cancer Lett* 2021;513:50–62.
20 Baryła I, Styczeń-Binkowska E, Płuciennik E, *et al*. The *WWOX/HIF1A* Axis Downregulation Alters Glucose Metabolism and Predispose to Metabolic Disorders. *Int J Mol Sci* 2022;23:3326.
21 Lencioni R, Llovet JM. Modified RECIST (mRECIST) assessment for hepatocellular carcinoma. *Semin Liver Dis* 2010;30:52–60.
22 Zhou C, Chen W, Sun J, *et al*. Low expression of WW domain-containing oxidoreductase associates with hepatocellular carcinoma aggressiveness and recurrence after curative resection. *Cancer Med* 2018;7:3031–43.
23 Aqeilan RI, Palamarchuk A, Weigel RJ, *et al*. Physical and functional interactions between the Wwox tumor suppressor protein and the AP-2gamma transcription factor. *Cancer Res* 2004;64:8256–61.
24 Qiu B, Li S, Li M, *et al*. KAT8 acetylation-controlled lipolysis affects the invasive and migratory potential of colorectal cancer cells. *Cell Death Dis* 2023;14:164.
25 Yu Z, Peng Y, Gao J, *et al*. The p23 co-chaperone is a succinate-activated COX-2 transcription factor in lung adenocarcinoma tumorigenesis. *Sci Adv* 2023;9:eade0387.
26 Fujita Y, Fujiwara K, Zenitani S, *et al*. Acetylation of NDPK-D Regulates Its Subcellular Localization and Cell Survival. *PLoS One* 2015;10:e0139616.
27 Ramos D, Aldaz CM. WWOX, a chromosomal fragile site gene and its role in cancer. *Adv Exp Med Biol* 2006;587:149–59.
28 Kuroki T, Yendamuri S, Trapasso F, *et al*. The tumor suppressor gene WWOX at FRA16D is involved in pancreatic carcinogenesis. *Clin Cancer Res* 2004;10:2459–65.
29 Mahajan NP, Whang YE, Mohler JL, *et al*. Activated tyrosine kinase Ack1 promotes prostate tumorigenesis: role of Ack1 in polyubiquitination of tumor suppressor Wwox. *Cancer Res* 2005;65:10514–23.
30 Abu-Remaileh M, Aqeilan RI. Tumor suppressor WWOX regulates glucose metabolism via HIF1α modulation. *Cell Death Differ* 2014;21:1805–14.
31 Iatan I, Choi HY, Ruel I, *et al*. The WWOX gene modulates high-density lipoprotein and lipid metabolism. *Circ Cardiovasc Genet* 2014;7:491–504.
32 Yang P, Su C, Luo X, *et al*. Dietary oleic acid-induced CD36 promotes cervical cancer cell growth and metastasis via up-regulation Src/ERK pathway. *Cancer Lett* 2018;438:76–85.
33 Ubellacker JM, Tasdogan A, Ramesh V, *et al*. Lymph protects metastasizing melanoma cells from ferroptosis. *Nature New Biol* 2020;585:113–8.
34 Wu H, Han Y, Rodriguez Sillke Y, *et al*. Lipid droplet-dependent fatty acid metabolism controls the immune suppressive phenotype of tumor-associated macrophages. *EMBO Mol Med* 2019;11:e10698.
35 Wei C-Y, Zhu M-X, Zhang P-F, *et al*. PKCα/ZFP64/CSF1 axis resets the tumor microenvironment and fuels anti-PD1 resistance in hepatocellular carcinoma. *J Hepatol* 2022;77:163–76.
36 Zhou C, Weng J, Liu C, *et al*. Disruption of SLFN11 Deficiency-Induced CCL2 Signaling and Macrophage M2 Polarization Potentiates Anti-PD-1 Therapy Efficacy in Hepatocellular Carcinoma. *Gastroenterology* 2023;164:1261–78.
37 Bouvard C, Lim SM, Ludka J, *et al*. Small molecule selectively suppresses MYC transcription in cancer cells. *Proc Natl Acad Sci U S A* 2017;114:3497–502.